

12;13

## Simulation of focused ion beam milling of multilayer substrates

© A.V. Rumyantsev, N.I. Borgardt, R.L. Volkov

National Research University of Electronic Technology, Zelenograd, Moscow, Russia

E-mail: lemi@miee.ru

Received February 21, 2023

Revised March 25, 2023

Accepted March 27, 2023

The level set method was generalized for simulating the evolution of the surface of multilayer substrates under focused ion beam irradiation. For a correct description of such process the calculations took into account the sputtering yield angular dependences, the densities of the irradiated materials and it was considered that sputtered atoms can escape from different layers of the substrate. Comparison of the calculation results with experimental data for test structures formed in a two-layer silicon dioxide–crystalline silicon substrate showed that the developed simulation method makes it possible to predict the shape of structures fabricated by a focused ion beam with good accuracy.

**Keywords:** Focused ion beam, sputtering, level set method.

DOI: 10.21883/TPL.2023.05.56035.19533

The focused ion beam (FIB) technique is currently used widely in various fields of science and technology (microelectronics included), since it provides an opportunity for direct precision fabrication and analysis of micro- and nanostructures on substrates made of almost any material, and specifically those consisting of several layers. FIB sputtering (etching) of multilayer structures is needed to solve a number of problems. Specifically, metal and dielectric layers may be used as solid masks that ensure high resolution and operation rate in the process of nanostructure formation with an FIB [1]. The modification of integrated microcircuits [2] and waveguides of semiconductor lasers [3] are practically relevant examples of the effect of an FIB on multilayer structures.

Computer modeling, which provides a quantitative description of the sample surface evolution under the influence of an ion beam, simplifies considerably the process of structure fabrication with an FIB, allowing one to minimize the application of resource-consuming trial-and-error techniques. The effect of an FIB on silicon [4,5] and silicon oxide [6] substrates was considered in the existing approaches to modeling of the shape of structures, including those utilizing the level set method. The results for multilayer structures are limited by analytical estimation of the depth of sputtering of a two-layer target [7] and Monte Carlo modeling of ion penetration combined with cell-based calculations of the sample surface evolution [8].

The aim of the present study is to further the application of the level set method in characterization of surface evolution of multilayer substrates under the influence of an FIB. The results of modeling of two types of test cavities formed in a silicon dioxide layer on the surface of crystalline silicon are compared with electron microscope images of cross sections of structures prepared in experiments.

If a substrate is subjected to FIB sputtering, distance  $z$  of the sample surface at point  $(x, y)$  from plane  $xOy$  at time  $t$

may be written as  $z = S(x, y, t)$  (Fig. 1). Surface  $S(x, y, t)$  is defined within the level set method as the zero level of function  $\Phi(x, y, z, t)$  that satisfies the following differential equation [9]:

$$\frac{\partial \Phi(\mathbf{r}, t)}{\partial t} + V_N(\mathbf{r}, t) |\nabla \Phi(\mathbf{r}, t)| = 0, \quad (1)$$

where  $\mathbf{r} = (x, y, z)$  and  $V_N(\mathbf{r}, t)$  is the rate of displacement of sample surface elements under the influence of an ion beam in the direction normal to them. This rate is set by the flux densities of atoms sputtered by an ion beam ( $F_{sp}(\mathbf{r}, t)$ ) and sputtered atoms redeposited onto the sample surface ( $F_r(\mathbf{r}, t)$ ).

Generalizing the known expression for  $F_{sp}(\mathbf{r}, t)$  [4] to the case of multilayer substrates and limiting ourselves (for

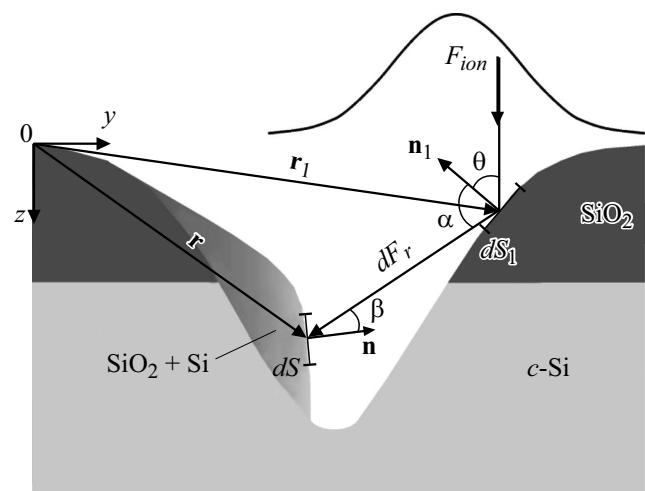


**Figure 1.** Schematic diagram of the process of sputtering of a substrate consisting of a silicon dioxide layer on the surface of crystalline silicon (*c*-Si).  $\mathbf{n}$  and  $\mathbf{n}_1$  are unit vectors normal to surface elements  $dS$  and  $dS_1$ , respectively.

simplicity) to two-layer structures, we find the following expression for the flux density of atoms sputtered from surface element  $dS_1$  with its center at point  $\mathbf{r}_1$ :

$$F_{sp}(\mathbf{r}_1, t) = \sum_{i=1,2} F_{sp,i}(\mathbf{r}_1, t), \quad (2)$$

where  $F_{sp,i}(\mathbf{r}_1, t)$  is the flux density of sputtered atoms of the  $i$ th material that is written as

$$F_{sp,i}(\mathbf{r}_1, t) = F_{ion}(\mathbf{r}_1) \cos \theta C_i(\mathbf{r}_1, t) Y_i(\theta) (1 + \mu_i), \quad (3)$$

where  $F_{ion}(\mathbf{r}_1)$  is the flux density of gallium ions;  $\mu_i = [Y_{r,i}(\theta)/Y_i(\theta) - 1]$  is a parameter that characterizes the difference between the rates of sputtering of the  $i$ th material in its redeposited and initial states and is defined by sputtering yields  $Y_{r,i}(\theta)$  and  $Y_i(\theta)$ , respectively;  $C_i(\mathbf{r}_1, t)$  is the fraction of the  $i$ th material in sputtered volume  $dV_1$  in the vicinity of point  $\mathbf{r}_1$ ; and angle  $\theta$  is determined in accordance with Fig. 1.

The flux density of atoms redeposited onto surface element  $dS$  located at point  $\mathbf{r}$  (Fig. 1) may be written as

$$F_r(\mathbf{r}, t) = \sum_{i=1,2} F_{r,i}(\mathbf{r}, t), \quad (4)$$

where  $F_{r,i}(\mathbf{r}, t)$  is the flux density of redeposited atoms of the  $i$ th material. If their angular distribution follows the cosine law, this flux density is determined by generalizing the expression from [4]

$$F_{r,i}(\mathbf{r}, t) = \frac{1}{\pi} \int \frac{F_{sp,i}(\mathbf{r}_1, t) \cos \alpha \cos \beta}{(\mathbf{r} - \mathbf{r}_1)^2} dS_1 \quad (5)$$

with angles  $\alpha$  and  $\beta$  determined in accordance with Fig. 1 and integrating over the entire region of beam-sample interaction.

Displacement rate  $V_N(\mathbf{r}, t)$  of surface element  $dS$  under the influence of an ion beam may be written as

$$V_N(\mathbf{r}, t) = \sum_{i=1,2} \frac{F_{sp,i}(\mathbf{r}, t) - \gamma F_{r,i}(\mathbf{r}, t)}{n_i}, \quad (6)$$

where  $\gamma$  is the „sticking“ coefficient that is the ratio of the number of atoms settling onto surface element  $dS$  to the overall number of sputtered atoms reaching this surface (in accordance with [4], this coefficient was set to unity) and  $n_i$  is the density of atoms of the  $i$ th material.

Flux density  $F_{ion}(x, y)$  of beam ions was represented in a well-accepted form of a sum of two Gaussian functions

$$F_{ion}(x, y) = \frac{I}{e} \frac{1}{2\pi(\sigma_1^2 + w\sigma_2^2)} \left[ \exp\left(-\frac{x^2 + y^2}{2\sigma_1^2}\right) + w \exp\left(-\frac{x^2 + y^2}{2\sigma_2^2}\right) \right] \quad (7)$$

with parameters  $\sigma_1 = 53$  nm,  $\sigma_2 = 136$  nm, and  $w = 0.08$ , which were determined using the approach detailed in [10].

Equation (1) was solved numerically on the primary regular rectangular computational mesh to determine  $\Phi(\mathbf{r}, t)$ . Function  $S(x, y, t)$  was determined based on  $\Phi(\mathbf{r}, t)$  at each time step using the marching cubes method and an irregular mesh of triangular elements [11]. Ion fluxes and displacement rates  $V_N(\mathbf{r}, t)$  were calculated on surface  $S(x, y, t)$  and were transferred via nearest-neighbor interpolation to the primary grid, where discretization of functions  $C_i(\mathbf{r}, t)$  was also performed, in order to solve (1).

Functions  $C_i(\mathbf{r}, t)$  at  $t = 0$  were specified by the two-layer structure of the substrate irradiated by an ion beam. If condition  $F_r > F_{sp}$  was satisfied in the vicinity of point  $\mathbf{r}$  for sputtered surface element  $\Delta S$ , the total number of redeposited atoms in a cell corresponding to  $\mathbf{r}$  with volume  $\Delta V$  varied by  $\Delta N = (F_r - F_{sp})\Delta S\Delta t$ , while the number of atoms of the  $i$ th material varied by  $\Delta N_i = (F_{r,i} - F_{sp,i})\Delta S\Delta t$ . To simplify the calculations, fluxes  $F_{sp,i}$  were determined using formula (3) without account for parameters  $\mu_i$  if the fraction of redeposited material in a cell was below 50%; when this fraction exceeded 50%, the parameter values were taken into account.

This method of modeling was implemented within a set of programs developed earlier [5]. The obtained results of numerical calculations were compared to experimental data for test structures formed with a Helios Nanolab 650 electron/ion microscope on single-crystal silicon substrates coated with a layer of thermal silicon dioxide with a thickness of approximately 600 nm. Structures were fabricated at an accelerating voltage of 30 kV and a beam current of  $I = 900$  pA with equal beam steps  $a = b = 38.5$  nm in perpendicular directions. Rectangular cavities  $1 \times 1 \mu\text{m}$  in size formed in  $N = 48$  beam passes with exposure time  $t_d = 0.1$  ms were the first type of structures. Structures of the second type were narrow grooves with a high aspect ratio. They were formed by moving an ion beam along straight lines with a length of approximately  $3 \mu\text{m}$  in  $N = 200$  passes with exposure time  $t_d = 0.2$  ms. This choice of  $N$  and  $t_d$  values in the fabrication of structures of both types provided an opportunity to illustrate the relevance of the proposed modeling method to typical experimental applications. Cross-section samples for scanning transmission electron microscopy (STEM) studies with a Titan Themis 200 microscope were prepared by the *in situ* lift out method [12] immediately after the fabrication of test structures. Structures were modeled in accordance with the experimental conditions of their fabrication. The data from [6] (for  $\text{SiO}_2$ ) and [14] (for Si) were used for the angular dependences of sputtering yields, the correctness of characterization of which affects the accuracy of modeling [13]; the values of parameters  $\mu_i$  were calculated in reliance on ratios  $Y_{r,1}/Y_1 \approx 1.15$  for  $\text{SiO}_2$  [6] and  $Y_{r,2}/Y_2 \approx 1.3$  for Si [5].

Figures 2, *a, b* present SEM (scanning electron microscopy) images of cavities, and the results of their modeling are shown in the insets. It follows from Figs. 2, *c, d* that the calculated profiles of cavities (white dashed curves) agree well with the STEM images of their cross sections.

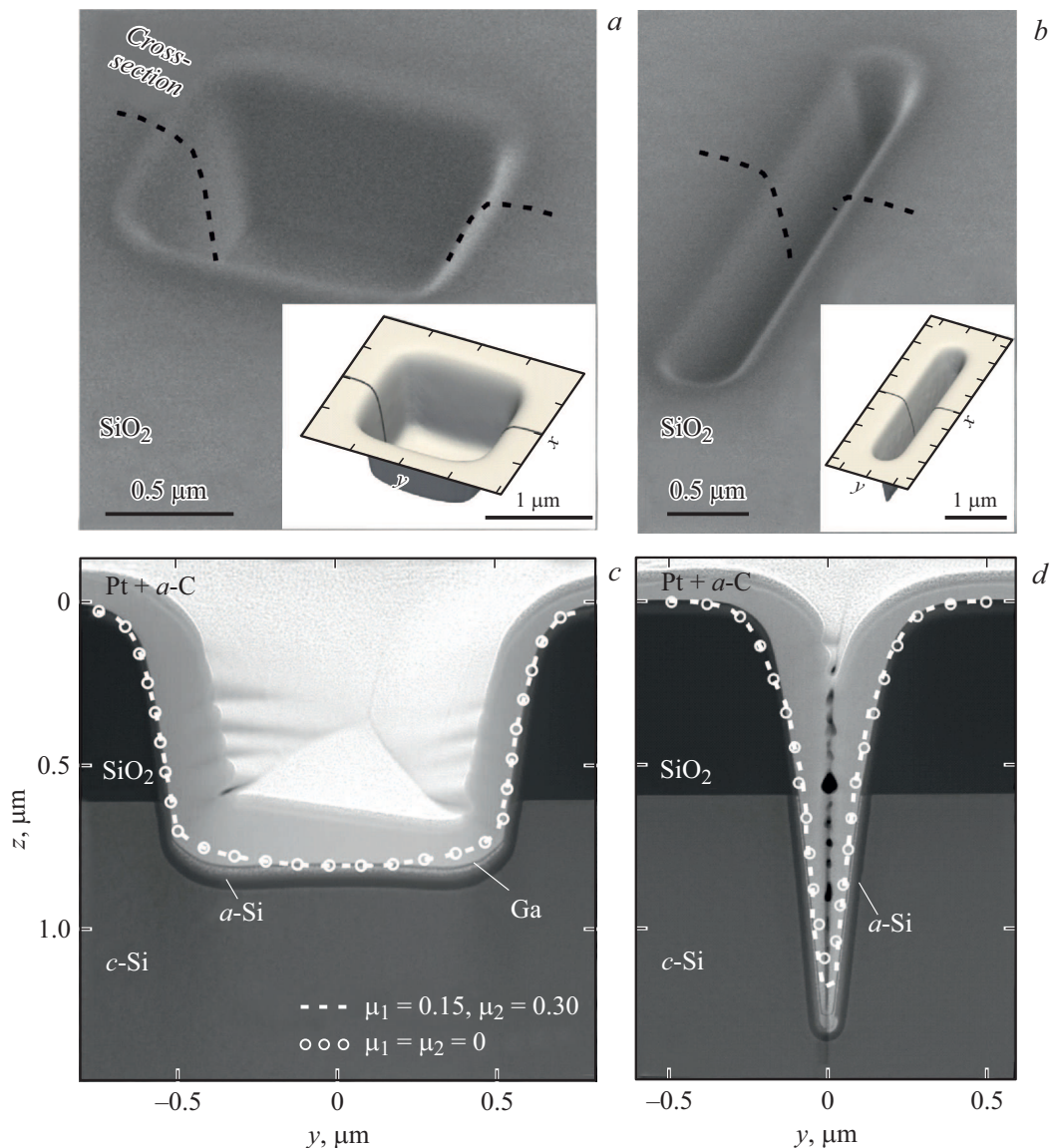


**Figure 2.** SEM (*a, b*) and STEM (*c, d*) images of rectangular cavities (*a, c*) and narrow grooves (*b, d*) formed by an FIB. The results of modeling of these cavities are shown in the insets in panels *a* and *b*. Profiles calculated both with (white dashed curves) and without (open circles) account for correct values of parameters  $\mu_1$  and  $\mu_2$  for SiO<sub>2</sub> and Si, respectively, are superimposed onto the STEM images of cavities in panels *c* and *d*. Cavities are coated with protective layers of platinum and amorphous carbon Pt + a-C; implanted gallium and amorphized silicon (a-Si) are visualized in their near-surface regions.

Slight discrepancies between the experimental and calculated data for rectangular cavities (Fig. 2, *c*) are apparently attributable to the reflection of incident ions from their side walls, which was neglected in modeling. The cross section of a narrow groove is V-shaped (Fig. 2, *d*), since the process of material redeposition plays a significant part in the formation of structures with a high aspect ratio. Open circles in Figs. 2, *c, d* denote the profiles obtained in modeling of cavities with no regard for an increase in the rate of sputtering of redeposited material. This omission is negligible in the case of a rectangular cavity (Fig. 2, *c*), since the amount of redeposited material is small; however, a closer agreement between the calculated and experimental

data for deep grooves (Fig. 2, *d*) is obtained when the mentioned increase in sputtering rate is taken into account.

Thus, the presented generalization of the level set method to the case of multilayer structures provided for efficient modeling of sputtering of a silicon substrate coated with a silicon dioxide layer by a focused ion beam. The introduction of angular dependences of sputtering yields for each of the substrate materials and the difference in their densities into calculations and a realistic description of the redeposition process made it possible to achieve a quantitative agreement between calculated and experimental data. Note that the discussed method may be used directly to model the process of sputtering of substrates with more

than two layers if data characterizing the interaction of an ion beam with the material of these layers are available.

### Funding

This study was supported financially by the Russian Science Foundation (agreement No. 21-79-00197).

### Conflict of interest

The authors declare that they have no conflict of interest.

### References

- [1] A.C. Madison, J.S. Villarrubia, K.T. Liao, C.R. Copeland, J. Schumacher, K. Siebein, B.R. Ilic, J.A. Liddle, S.M. Stavis, *Adv. Funct. Mater.*, **32** (38), 2111840 (2022). DOI: 10.1002/adfm.202111840
- [2] S. Herschbein, S. Tan, R. Livengood, M. Wong, in *Proc. of the ISTFA-2022* (Pasadena, California, USA, 2022), p. i1-i69. DOI: 10.31399/asm.cp.istfa2022tpi1
- [3] A.S. Payusov, M.I. Mitrofanov, G.O. Kornyshev, A.A. Serin, G.V. Voznyuk, M.M. Kulagina, V.P. Evtikhiev, N.Yu. Gordeev, M.V. Maximov, S. Breuer, *Tech. Phys. Lett.*, **48** (15), 87 (2022). DOI: 10.21883/TPL.2022.15.54275.18980.
- [4] H.B. Kim, G. Hobler, A. Steiger, A. Lugstein, E. Bertagnolli, *Nanotechnology*, **18** (26), 265307 (2007). DOI: 10.1088/0957-4484/18/26/265307
- [5] N.I. Borgardt, R.L. Volkov, A.V. Rumyantsev, Yu.A. Chaplygin, *Tech. Phys. Lett.*, **41** (6), 610 (2015). DOI: 10.1134/S106378501506019X.
- [6] A.V. Rumyantsev, N.I. Borgardt, R.L. Volkov, Yu.A. Chaplygin, *Vacuum*, **202**, 111128 (2022). DOI: 10.1016/j.vacuum.2022.111128
- [7] A.A. Tseng, I.A. Insua, J.S. Park, C.D. Chen, *J. Micromech. Microeng.*, **15** (1), 20 (2004). DOI: 10.1088/0960-1317/15/1/004
- [8] W. Boxleitner, G. Hobler, *Nucl. Instrum. Meth. Phys. Res. B*, **180** (1-4), 125 (2001). DOI: 10.1016/S0168-583X(01)00406-2
- [9] F. Gibou, R. Fedkiw, S. Osher, *J. Comput. Phys.*, **353**, 82 (2018). DOI: 10.1016/j.jcp.2017.10.006
- [10] N.I. Borgardt, A.V. Rumyantsev, *J. Vac. Sci. Technol. B*, **34** (6), 061803 (2016). DOI: 10.1116/1.4967249
- [11] P. Manstetten, J. Weinbub, A. Hössinger, S. Selberherr, *Proc. Comput. Sci.*, **108**, 245 (2017). DOI: 10.1016/j.procs.2017.05.067
- [12] L.A. Giannuzzi, F.A. Stevie, *Micron*, **30** (3), 197 (1999). DOI: 10.1016/S0968-4328(99)00005-0
- [13] V.I. Bachurin, I.V. Zhuravlev, D.E. Pukhov, A.S. Rudy, S.G. Simakin, M.A. Smirnova, A.B. Churilov, *J. Surf. Investig.*, **14** (4), 784 (2020). DOI: 10.1134/S1027451020040229.
- [14] L. Frey, C. Lehrer, H. Ryssel, *Appl. Phys. A*, **76** (7), 1017 (2003). DOI: 10.1007/s00339-002-1943-1

*Translated by D.Safin*